

Molybdenum-Catalyzed Olefin Epoxidation: Ligand Effects**

Werner R. Thiel* and Jörg Eppinger

Abstract: We synthesized substituted pyrazolylpyridine ligands to examine their donor properties by spectroscopic (IR, NMR) and computational (AM1) methods. The influence of the substitution patterns on spectroscopic and thermodynamic features of molybdenum oxobisperoxo complexes $[(L-L)MoO(O_2)_2]$ ($L-L = 2-(1-alkyl-3-pyrazolyl)pyridine/pyrazine$) correlates with the activities of the complexes in catalytic olefin epoxidation reactions. This further proof for the relation between the Lewis acidity and the catalytic activity of epoxidation catalysts supports a reaction mechanism in which the peroxo complex activates the oxidizing agent (H_2O_2 , ROOH) instead of directly transferring an oxygen atom from a η^2 -peroxo ligand to the olefin.

Keywords
catalysis · epoxidations · molybdenum · olefins · peroxo complexes

Introduction

High-valent molybdenum complexes are known as highly active catalysts for the epoxidation of olefins in the presence of peroxidic reagents like hydrogen peroxide or alkyl hydroperoxides.^[2] During the last two decades, systems with alkoxo, peroxo, acetato, acetylacetonato, halogeno, or oxo ligands have been investigated,^[3] but the chemical constitution of the active species often remained the subject of speculation. In the case of $[Mo(CO)_6]$, for example, which exhibits catalytic activity only after a period of activation, all we currently know about the mechanism is that the low-valent carbonyl complex is oxidized, resulting in the formation of alcoholato complexes, which have not been structurally characterized yet.^[4]

The dearth of structurally well-defined molybdenum(VI) catalysts for olefin epoxidation encouraged us to study Mimoun-type^[5] molybdenum oxobisperoxo complexes $[(L-L)MoO(O_2)_2]$, in which $L-L$ is a bidentate 2-(1-alkyl-3-pyrazolyl)pyridine ligand.^[6] From earlier investigations, we knew that these complexes are not subject to ligand exchange reactions under catalytic conditions. Their coordinative stability and their excellent solubility in organic solvents make these peroxo complexes perfect candidates for spectroscopic investigations into the mechanism of catalytic olefin epoxidation. As shown in a previous paper, the oxygen atom transferred to the olefin does not originate from one of the η^2 -peroxo ligands, but from the oxidizing agent.^[7] These results confirm the activation of *t*BuOOH by the Lewis acidic peroxo complexes as a key step in the catalytic cycle.

In this paper we describe the influence of either electron-withdrawing or -donating substituted ligands on the catalytic activities of the molybdenum oxobisperoxo complexes mentioned above. Pyrazolylpyridines prove to be ideal ligands for that kind of inquiry, since substitution reactions at the pyrazole as well as at the pyridine moiety allow the modification of the donor strength of the chelate system.

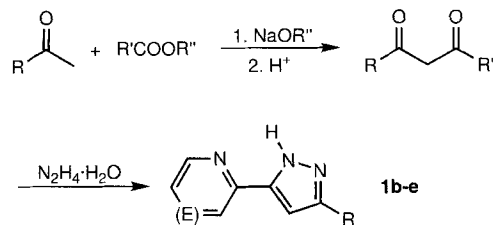
Results and Discussion

The chemistry of pyrazole and its derivatives is well established.^[8] A multitude of synthetic routes has been worked out during the last decades, as some members of the pyrazole family play an economically important role in pharmacy and agrochemistry.^[9] In a straightforward synthesis, Claisen condensation of a (mono)alkyl ketone with a carboxylic ester results in the formation of a 1,3-diketone, which can be converted to the corresponding pyrazole by a ring closure reaction with hydrazine. Following this route, Brunner et al. obtained 2-(3(5)-pyrazolyl)pyridine (**1a**) from acetylpyridine, *N,N*-dimethylformamide dimethylacetal, and hydrazine.^[10] We synthesized the derivatives **1b–d** by variation of either the ketone or the carboxylic ester.^[11] Use of pyrazine carboxylic acid ester instead of the picolinic derivative yielded the corresponding 2-(3(5)-pyrazolyl)pyrazine **1e** (Scheme 1).^[12] On the other hand, pyrazoles easily undergo electrophilic substitutions in the 4-position.^[8, 13] This feature was applied in the syntheses of the chloro, bromo, and nitro derivatives **1f–h** (Scheme 2).

For a first survey of the influence of the substitution patterns on the electronic situation of the ligands **1a–h**, and thus on their donor properties, we investigated the N–H stretching vibrations of these compounds by IR spectroscopy as well as by computational methods.^[14] Formally, 2-(3-pyrazolyl)pyridines can exist in three tautomeric forms **A–C**.^[15] Additionally, a

[*] Dr. W. R. Thiel, Dipl.-Chem. J. Eppinger
Anorganisch-chemisches Institut, Technische Universität München
Lichtenbergstr. 4, D-85747 Garching
Fax: Int. code + (89) 3209-3473
e-mail: thiel@arthur.anorg.chemie.tu-muenchen.de

[**] Metal-Catalyzed Oxidations. Part 6. Part 5: Ref. [1].



- 1b:** R = CH₃, R' = *o*-C₅H₄N, R'' = CH₃, E = CH
1c: R = C₆H₅, R' = *o*-C₅H₄N, R'' = CH₃, E = CH
1d: R = *o*-C₅H₄N, R' = CF₃, R'' = C₂H₅, E = CH
1e: R = CH₃, R' = C₄H₃N₂, R'' = C₂H₅, E = N

Scheme 1. Synthesis of the 2-(3-pyrazolyl)pyridines **1b–e**.

- 1f:** Y = Cl; **1g:** Y = Br; **1h:** Y = NO₂

Scheme 2. Synthesis of the 2-(3-pyrazolyl)pyridines **1f–h**.

(small) barrier for the rotation around the pyrazolyl–pyridine bond should be taken into account.^[16] Therefore, six different geometries had to be minimized for each ligand **1a–h** in a computational study (Figure 1). Solvent- and temperature-dependent NMR spectra with broad signals, especially for N–H protons, suggest an equilibrium between tautomers/rotamers in solution. For the computational optimization of the geometries and the calculation of thermodynamic data for these species, dihedral angles N2–C–C–N3 of 160° for the tautomers **A1**, **B1**, and **C1** and of 20° for the corresponding rotamers **A2**, **B2**, and **C2** were chosen as starting conditions (for atom numbering see Figure 1). As the most important result of our calculations on the systems **1a–h** we found that generally **B2** is the thermodynamically most stable form (Table 1). It is stabilized by a dipole–dipole interaction between the N2 proton and the lone

Abstract in German: Mehrere substituierte Pyrazolylpyridinliganden wurden synthetisiert und ihre Donoreigenschaften durch spektroskopische Methoden (IR, NMR) und semiempirische Rechnungen (AM1) untersucht. Dabei zeigte sich, daß sich der elektronische Einfluß der Substituenten an den Liganden eindeutig mit spektroskopischen und thermodynamischen Daten der entsprechenden Oxobisperoxomolybdänkomplexe [(L–L)–MoO(O₂)₂] (L–L = 2-(1-Alkyl-3-pyrazolyl)pyridin/pyrazin), und deren katalytischer Aktivität bei der Olefinepoxidierung korrelieren läßt. Dies ist ein wichtiger Hinweis auf den Zusammenhang zwischen der Lewis-Acidität von Epoxidierungskatalysatoren und ihrer katalytischen Aktivität. Des weiteren stützen diese Ergebnisse eine über die Aktivierung des Oxidationsmittels durch die Lewis-aciden Peroxo-Komplexe verlaufende Sauerstoffübertragung auf das Olefin, und nicht einen direkten Sauerstofftransfer von einem η²-koordinierten Peroxoliganden.

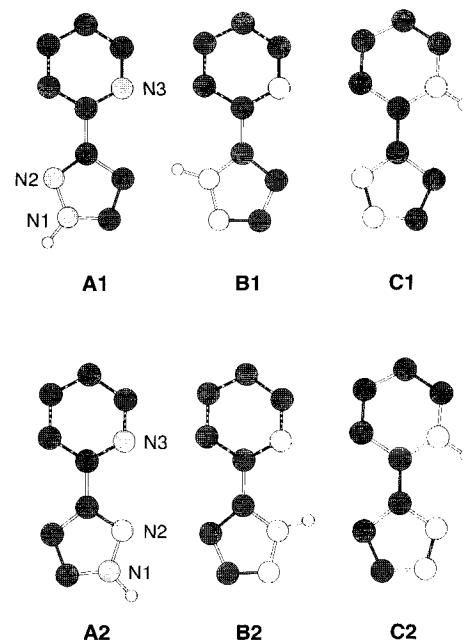


Figure 1. Six isomeric structures of 2-(3-pyrazolyl)pyridine (rotamers/tautomers).

Table 1. Calculated (AM1) relative heats of formation $\Delta\Delta G$ [kJ mol⁻¹] (with respect to **B2**) and torsion angles N2–C–C–N3 [°] of the six isomeric geometries of **1a–h**.

		1a	1b	1c	1d	1e	1f	1g	1h
A1	$\Delta\Delta G$	13.49	9.54	8.80	17.27	6.67	15.44	15.34	18.09
	torsion	178	179	179	177	180	149	137	130
B1	$\Delta\Delta G$	13.49	13.74	13.64	14.39	13.35	12.94	12.61	14.56
	torsion	161	161	164	159	165	148	137	121
C1	$\Delta\Delta G$	75.82	71.34	67.76	62.74	73.84	61.05	62.57	44.22
	torsion	180	180	180	180	180	180	180	163
A2	$\Delta\Delta G$	17.83	13.85	13.37	22.09	10.88	16.84	15.14	18.57
	torsion	30	30	29	31	26	47	54	50
B2	$\Delta\Delta G$	0	0	0	0	0	0	0	0
	torsion	0	0	2	1	0	22	30	35
C2	$\Delta\Delta G$	65.37	61.24	57.44	51.48	64.24	60.23	62.63	58.12
	torsion	0	0	0	0	0	0	0	23

pair of N3. An analogous stabilization could be found for **C2** compared with **C1** (**1a–e**: $\Delta G_{(C2, C1)}$ ca. 10 kJ mol⁻¹). This particular stabilization can be canceled out if the steric demand of substituents in the 4-position of the pyrazole moiety hampers a coplanar arrangement of the ring systems (**1f,g**). In the case of **1h** a strong dipole–dipole interaction between the 4-nitro substituent and the N3 proton is responsible for the stabilization of **C1** compared to **C2**.

In the absence of bulky substituents in the 4-position of the pyrazole ring (ligands **1a–e**), four of the six tautomers/rotamers (**A1**, **C1**, **B2**, **C2**) show an almost coplanar arrangement of both rings, while for the two other geometries (**B1**, **A2**) interplanar angles of 20–30° are calculated. In the case of these two isomers, a relatively high degree of steric hindrance (H–H interaction) cannot be compensated by π or dipole–dipole interactions. Substitution of the pyrazole proton in the 4-position by more sterically demanding groups (**1f–h**) leads to nonplanar geometries for **A1**, **B1**, **A2**, and **B2**, but **C1** and **C2** remain planar in the case of **1f,g**; this can be explained by rather strong dipole–dipole interactions.

However, a coplanar arrangement of the ring systems is necessary for chelating coordination to a metal center. For this reason, beside electronic effects, a substituent at the 4-position of the pyrazole ring should weaken the metal–ligand interaction and therefore increase the Lewis acidity of the metal center.

Calculation of all six N–H stretching frequencies (tautomers/rotamers **A1–C2**) for every ligand **1a–h** gave a deeper insight into the electronic influence of the substitution patterns on the donor properties of the ligands. Electron-withdrawing substituents, which stabilize the deprotonated (anionic) form and weaken the N–H bond, should shift the N–H absorption to lower wavenumbers. IR experiments in solution resulted for all ligands except **1b** in only one N–H absorption. As shown in Table 2 and Figure 2, the experimental data agree quite well

Table 2. Calculated (AM1, six geometries) and experimental N–H stretching frequencies [cm^{-1}] for the ligands **1a–h**.

	1a	1b	1c	1d	1e	1f	1g	1h
A1	3484.4	3484.2	3475.2	3451.4	3478.7	3476.0	3474.2	3452.3
B1	3483.1	3483.4	3478.2	3459.0	3479.0	3474.7	3473.4	3451.8
C1	3440.2	3441.4	3438.6	3424.1	3447.9	3319.6	3254.4	3292.5
A2	3481.6	3481.8	3473.1	3448.0	3477.7	3473.5	3472.2	3448.1
B2	3453.9	3451.9	3448.1	3427.0	3452.3	3445.3	3446.9	3425.1
C2	3406.0	3409.4	3404.3	3386.3	3415.5	3392.4	3390.7	3361.5
$\bar{\nu}_{\text{obs}}$	3445	3444	3437	3421	3443	3429	3427	3401
		(3511)						

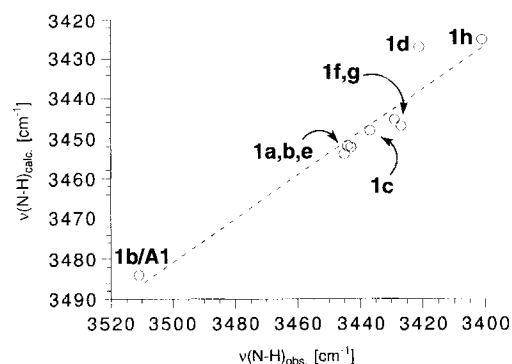
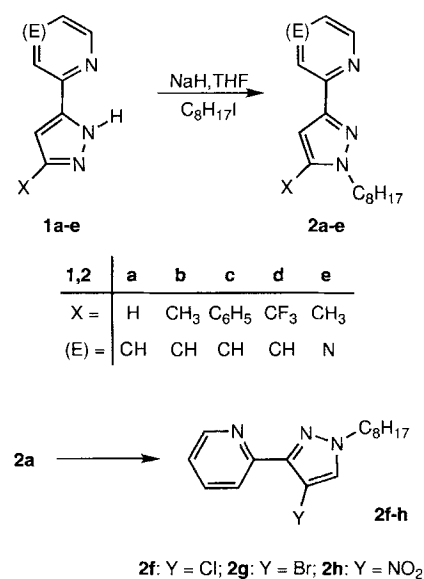


Figure 2. Correlation of calculated and experimental N–H stretching frequencies of the tautomer **B2** (compounds **1a–h**) and tautomer **A1** of **1b**.

with the calculated N–H absorptions of the tautomeric form **B2** ($R = 0.958$). Nevertheless, solvent or concentration effects might influence the experimental values. Together with the thermodynamic data in Table 1, these experiments confirm that **B2** is indeed the major tautomer/rotamer in solution. Only in the case of **1b** can a second N–H absorption with low intensity be observed. From a thermodynamic point of view, it is obvious that the electron-donating methyl group in the 5-position of the pyrazole ring stabilizes the tautomer **A1**. The N–H stretching frequency, which was calculated for **1b A1**, again matches with the experimental value. The influence of different substituents on $\nu(\text{N–H})$ could merely be correlated with their Hammett parameters, which are well established only for phenyl derivatives,^[17] but clearly the thermodynamic and spectroscopic properties can be interpreted mainly by inductive effects of the substituents.

Obviously, IR spectroscopy as well as semiempirical calculations are effective tools for the examination of substituent effects in pyrazoles.

We have shown in preceding papers that pyrazolopyridines with long alkyl side chains are useful ligands for the spectroscopic investigation of seven-coordinate molybdenum peroxo complexes, as they dramatically increase the solubility of these compounds.^[18] Olefin epoxidation reactions can thus be carried out in nonpolar organic solvents like *n*-hexane or toluene, leading to high yields of sensitive epoxides. The ring opening (side-)reaction of the epoxide is suppressed in these systems. Therefore, synthesis of the *N*-octyl derivatives of **1a–h** seemed to be worthwhile. While the *N*-octylated compounds **2a–e** could be obtained by reaction of **1a–e** with NaH in THF, followed by the addition of octyl iodide, electrophilic substitution of **2a** (after *N*-alkylation of **1a**) with either chlorine, bromine or nitric acid resulted in higher yields of **2f–h** (Scheme 3).

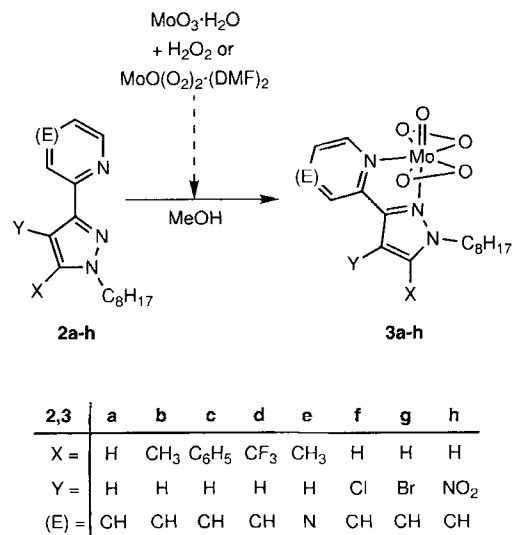


Scheme 3. Synthesis of the *N*-octylated 2-(3-pyrazolyl)pyridines **2a–h**.

The results of the alkylation reaction do not seem to coincide with the stability of the tautomer **B2**. This contradiction can be elucidated by taking into account the fact that deprotonation of the pyrazolopyridines with NaH leads to the corresponding anions, which certainly coordinate to the large (with respect to H⁺) sodium cation in a chelating manner. Therefore a nucleophilic attack on the octyl iodide can only proceed by N1 as long as the coordination of the ligand to Na⁺ is strong enough. Only in the case of **1d** (CF₃ substituent) could traces of a second compound be observed by GC/MS, showing an almost identical mass spectrum to **2d**. It seems that the electron-withdrawing effect of the CF₃ group leads to a weaker metal–ligand interaction and therefore to a (minor) alkylation at N2. As we do not observe any alkylation at N2 in the case of the other 5-substituted derivatives **1b,c,e**, we do not suggest that the regioselectivity of the alkylation is a result of steric hindrance by the *ortho* substituent pyridine/pyrazine in this position.

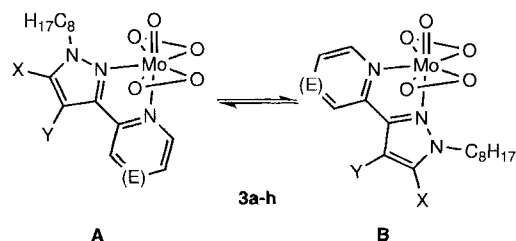
The molybdenum peroxo complexes **3a–h** can easily be obtained by stirring a methanolic solution of the corresponding

ligand with an excess of hydrated molybdenum oxide ("molybdic acid") in dissolved hydrogen peroxide or by ligand exchange with $[\text{MoO}(\text{O}_2)_2 \cdot (\text{DMF})_2]$ as source of the molybdenum peroxy unit (Scheme 4).



Scheme 4. Synthesis of the molybdenum peroxy complexes **3a–h**.

Owing to the asymmetric nature of the ligand featuring two different coordinating nitrogen donor centers, these peroxy complexes exist in two isomeric forms **A** and **B**, which differ in the orientation of the aromatic rings relative to the axial oxo ligand. In isomer **A** the pyridine ring occupies the second axial position in the same manner as the pyrazole ring in isomer **B**. From spin exchange experiments with **3a** we know that the isomers are in equilibrium in solution (Scheme 5).^[19] Therefore the isomer ratio is not kinetically but thermodynamically deter-



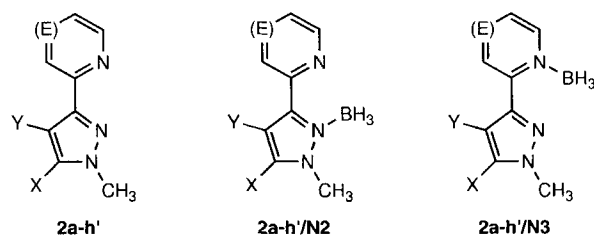
Scheme 5. Equilibrium of the two isomers **A** and **B** of **3a–h**.

Table 3. Calculated (AM1) dissociation energies ($\Delta G_{\text{N}2}$, $\Delta G_{\text{N}3}$, $\Delta\Delta G_{\text{N}3-\text{N}2}$) of the BH_3 adducts of **2a–h'** (coplanar geometry), calculated partial charges on the BH_3 fragment, and B–N distances ($d_{\text{B-N}}$) for **2a–h'/N2** and **2a–h'/N3**.

Ligand	Subst.	$\Delta G_{\text{N}2}$ Calcd. [kJ mol ⁻¹]	$\Delta G_{\text{N}3}$ Calcd. [kJ mol ⁻¹]	$\Delta\Delta G_{\text{N}2-\text{N}3}$ Calcd. [kJ mol ⁻¹]	2a–h'/N2		2a–h'/N3	
					Part. charge on BH_3	$d_{\text{B-N}2}$ [Å]	Part. charge on BH_3	$d_{\text{B-N}3}$ [Å]
2a'	CH/4,5-H	58.941	77.516	-18.576	-0.3167	1.600	-0.3629	1.590
2b'	CH/5-CH ₃	58.666	77.968	-19.302	-0.3182	1.601	-0.3639	1.590
2c'	CH/5-Ph	56.904	77.595	-20.691	-0.3163	1.601	-0.3632	1.590
2d'	CH/5-CF ₃	47.417	75.319	-27.901	-0.2936	1.608	-0.3596	1.591
2e'	N/5-CH ₃	57.861	74.175	-16.314	-0.3161	1.600	-0.3502	1.584
2f'	CH/4-Cl	51.179	74.111	-22.933	-0.3058	1.610	-0.3622	1.593
2g'	CH/4-Br	50.811	73.848	-23.036	-0.3057	1.610	-0.3617	1.593
2h'	CH/4-NO ₂	38.952	67.091	-28.140	-0.2851	1.624	-0.3552	1.597

mined. The preferred orientation of the pyridine moiety *trans* to the oxo ligand in **3a** can be explained as a consequence of the better σ donor properties of this fragment compared to pyrazole. Obviously, substitution at both donor systems will have an influence on the equilibrium illustrated in Scheme 5.

Calculations of the donor properties of N2 and N3 were performed for the N1-methylated model ligands **2a'–h'** (Scheme 6). We focused on species derived from the type **A2**



Scheme 6. Molecular structures of the model ligands **2a'–h'**. The BH_3 adducts **2a'–h'/N2** and **2a'–h'/N3** were used for calculation of dissociation energies.

(Figure 1), which were calculated in a fixed coplanar orientation of the heteroaromatic rings, since this geometry best matches that of the coordinated ligand in **3a–h**. Besides, the results of the calculations depend on the interplanar angle between the pyrazole and the pyridine fragment, because of π interactions between the heteroaromatic rings. In order to determine the donor properties of N2 and N3, dissociation energies of the corresponding BH_3 adducts **2a'–h'/N2** and **2a'–h'/N3** (Scheme 6, Table 3) were calculated.

According to the known basicities of 1-methylpyrazole and pyridine^[20] the formation of the BH_3 adduct at the pyridine site is thermodynamically favored; this is confirmed by the differences ($\Delta\Delta G_{\text{N}2-\text{N}3}$) of the dissociation energies $\Delta G_{\text{N}2}$ and $\Delta G_{\text{N}3}$ of the particular adducts. The calculations clearly show the influence of electron-withdrawing and -donating substituents on adduct formation. Additionally, the substitution patterns also determine charge distributions in the molecules, for example, on the BH_3 fragments, and the lengths of the B–N bonds, especially those of the B–N2 bonds (Table 3).

Nevertheless, characterizing the chelate ligands **2a–h** as a geometrically fixed arrangement of two independent donor centers would not be consistent with the results of our calculations. Electron-withdrawing groups, such as on the pyrazole moiety, also destabilize the $\text{BH}_3\text{-N}_3$ adduct. This can be explained in terms of the π interactions between both ring systems being coplanar (as in chelate complexes). These facts have to be kept in mind for the following discussion of the particular Lewis acidities of the peroxo complexes **3a–h**.

However, the equilibrium constants for the reactions $\text{A} \rightleftharpoons \text{B}$ (of **3a–h**) should only depend on the relative donor strengths of N_3 and N_2 . An almost linear relation ($R = 0.955$) can be obtained between the calculated $\Delta\Delta G_{\text{N}_2\text{-N}_3}$ and ΔG_{Mo} ($\Delta G_{\text{Mo}} = -RT \ln([A]/[B])$), determined by ^1H NMR spectroscopic measurements (Table 4, Figure 3). Consequently, the combination of spectroscopic data with theoretical calculations allows a qualitative description of some characteristics of these catalytically relevant transition metal complexes.

Table 4. Calculated dissociation energies $\Delta\Delta G_{\text{N}_3\text{-N}_2}$ and equilibrium constants $K_{\text{N}_3/\text{N}_2}$ of the BH_3 adducts of **2a'–h'**, and experimental (NMR) isomer ratios (A:B) and energy differences ΔG_{Mo} of the peroxo complexes **3a–h**.

Ligand	Subst.	$K_{\text{N}_3/\text{N}_2}$ calcd.	$\Delta\Delta G_{\text{N}_2\text{-N}_3}$ calcd. [kJ mol $^{-1}$]	Isomer ratio A:B	ΔG_{Mo} exp. [kJ mol $^{-1}$]
2a'	CH/4,5-H	1803	-18.576	1.71	-1.329
2b'	CH/5- CH_3	2417	-19.302	0.98	0.050
2c'	CH/5-Ph	4236	-20.691	1.42	-0.869
2d'	CH/5- CF_3	77764	-27.901	28.9	-8.334
2e'	$\text{N}_2/5\text{-CH}_3$	724	-16.314	0.084	6.137
2f'	CH/4-Cl	10470	-22.933	7.05	-4.839
2g'	CH/4-Br	10914	-23.036	7.86	-5.108
2h'	CH/4- NO_2	85639	-28.140	> 50	< -9.7

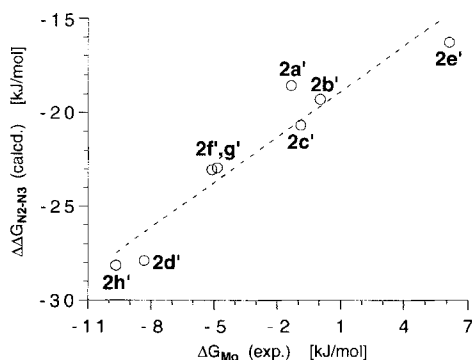


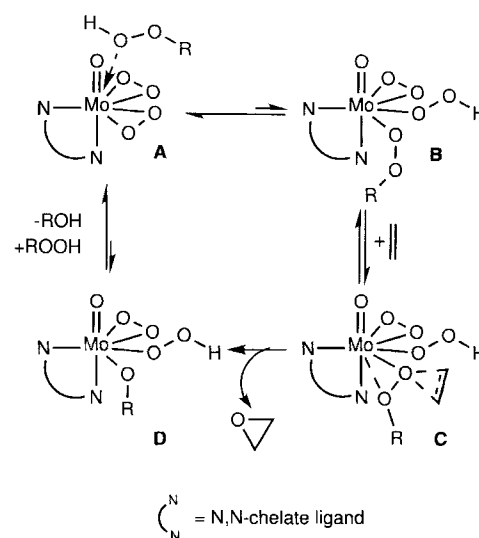
Figure 3. Correlation of calculated (**2a'–h'**) and experimental (**3a–h**) ΔG values.

In the case of the most electron-deficient pyrazole moiety (**3h**, nitro substituted), isomer **B** could not be observed at all. In contrast, complex **3e** shows an “inverse” isomer ratio, where the methyl substituent increases the electron density of the five-ring system, while the exchange of pyridine for pyrazine leads to the opposite effect for the six-ring heteroaromatic fragment.

Not only are the spectroscopic properties of the peroxo complexes **3a–h** influenced by their specific ligand substitution pattern, but also their epoxidation activities should depend on the electronic structure of the chelating ligand. As a result of mechanistic investigations we know that in the case of these seven-

coordinate complexes, the oxygen atom transferred to the olefin originates from the oxidizing agent $t\text{BuOOH}$ and not from a $\eta^2\text{-O}_2$ ligand of the peroxo complexes.^[7, 21] The activation of the hydroperoxide by a high-valent metal center is achieved through an interaction between the Lewis acidic metal complex and the Lewis basic hydroperoxide,^[22] promising highly active complexes bearing (chelate) ligands with electron-withdrawing substituents.

In the first step of the proposed reaction mechanism, the hydroperoxide coordinates to the peroxo complex, followed by a proton transfer reaction (Scheme 7). η^2 -coordination of the hydroperoxide to the Lewis acidic metal center activates the oxidizing agent towards electrophilic attack at the olefinic double bond. Reprotonation of the resulting alcoholato ligand and dissociation of the alcohol regenerates the ligand sphere of the oxobisperoxo complexes.



Scheme 7. Proposed mechanism for the catalytic olefin epoxidation by seven-coordinate molybdenum oxobisperoxo complexes of type **3a–h**.

In the case of our molybdenum oxobisperoxo complexes **3a–h**, the situation is even more complicated, because they exist in two isomeric forms in equilibrium at room temperature. It must be considered that all the other species involved in the mechanism can also show this structural feature. At present, we do not know anything about the equilibria between these isomers and their particular contribution to the overall activity of the catalytic system. We have just started a detailed NMR study on the coordination chemistry and ligand fluxionality of the complexes **3a–h**.

From catalytic epoxidations carried out at various temperatures we found a temperature-dependent activation period wherein the actual catalytically active species is formed. This catalyst species is therefore not identical with the oxobisperoxo molybdenum complex. We assume it to be a hydroperoxo alkylperoxo molybdenum complex as suggested in Scheme 7, but spectroscopic or structural evidence for this species is still lacking. At reaction temperatures above 50°C the activation periods of the complexes **3a–h** are too short to be observed by GC analysis, indicating that the reaction rates determining the

first equilibrium of the mechanism (formation of ROOMoOOH from Mo(η^2 -O₂) and ROOH) are high. Under these conditions the oxygen transfer from the active species to the olefin is the rate-determining step at the beginning of the reaction. For a qualitative description of the actual epoxidation activities of complexes **3a–h**, the initial turnover frequencies (TOF, Table 5) were calculated. Cyclooctene was used as the standard system.

Table 5. Experimental initial TOFs for the catalytic epoxidation of cyclooctene with the oxobisperoxo complexes **3a–h** (for conditions see Experimental Part), and their relative reactivities with respect to **3a**.

Complex	TOF [h ⁻¹]	Rel. Activity
3a	3420	1.00
3b	3160	0.92
3c	4040	1.18
3d	5710	1.67
3e	4940	1.45
3f	4930	1.44
3g	5200	1.52
3h	6470	1.89

In addition to the spectroscopic and thermodynamic features, the substitution pattern of the chelating ligand also controls the catalytic activity of the peroxo complexes **3a–h**. Electron-withdrawing groups, which elevate the Lewis acidity of the catalyst, are responsible for an increase in activity. In comparison to **3a**, the nitro substituent of **3h**, for example, increases the reactivity of this compound by a factor of almost two, while the methyl substituent in **3b** decreases its reactivity to 90%. Interestingly enough, substitution of pyrazine for the pyridine system overrules the influence of the methyl group at the pyrazole ring and leads to a higher reactivity of **3e**. Both the linear plot of the ΔG values and the logarithmic plot of the isomer ratios of **3a–h** (derived from NMR spectroscopy) against the reactivity data (see Figure 4) result in a linear correlation ($R = 0.979$) for the pyrazolypyridine complexes **3a–d** and **3f–g**. Obviously, the data for the pyrazine derivative **3e** cannot be correlated this way.

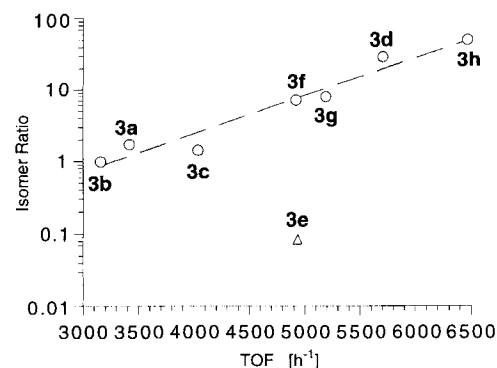


Figure 4. Logarithmic correlation of the initial TOFs and the isomer ratios of the peroxo complexes **3a–h**.

Thus the isomer ratios and the corresponding ΔG values for the complexes correlate with the donor properties of the particular ligands. Consequently, the electronic properties of the ligands determine the activities of the complexes **3a–h**. Steric effects should only play a minor role.

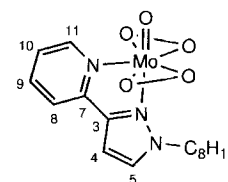
Conclusion

With a combination of spectroscopic, computational, and kinetic methods, we are now able to quantify the electronic influence of ligands on the activity of epoxidation catalysts. On the basis of the results, rules for the ligand design of epoxidation catalysts can be established. As mentioned in previous papers, coordinative stability of the catalytically active complexes and stability against oxidative degradation of the ligand system could be achieved by application of neutral chelate ligands bearing two nitrogen donor centers as parts of aromatic ring systems. The most simple and familiar ligand fulfilling these demands is 2,2'-bipyridine. Owing to the low solubility of bipyridine complexes of high-valent metal centers in organic solvents, a further structural feature for an optimal ligand (for catalysis in homogeneous systems) is required: alkyl side chains lead to increased solubility of the catalysts. Synthetic considerations directed us towards the pyrazolypyridine system, the donor properties of which can easily be optimized. As shown above, exchange of the pyridine for a less electron-rich pyrazine moiety results in increased activity in olefin epoxidation. Analogously, the introduction of a second pyrazolyl fragment instead of the pyridyl ring will improve the catalytic activity and allow further introduction of electron-withdrawing substituents. Our future research will concentrate on the synthesis of electron-deficient bispyrazolyl ligands in which the nitrogen bears -CH₂COOR moieties instead of electron-rich alkyl groups. These substituents have already proved to be ideal side chains with which to increase the catalytic activity of our peroxo complexes.^[6]

Experimental Section

General information: Ligands were prepared under nitrogen atmosphere; solvents were dried and distilled before use. 2-(3(5)-pyrazolyl)pyridine (**1a**),^[10] 2-(1-octyl-3-pyrazolyl)pyridine (**2a**),^[6] (1-octyl-3-pyrazolyl)pyridineoxodiperoxomolybdenum(vi) (**3a**),^[6] and [MoO(O₂)₂(DMF)₂]^[5] were synthesized as described in the literature. The NMR (Bruker DPX 400), mass (gas chromatograph Hewlett–Packard HP 5890 coupled with a mass-selective detector HP 5970, Finnigan MAT 90), and infrared spectra (Perkin–Elmer 1600 series FTIR), and all elemental analyses were carried out at the Anorganisch-chemisches Institut der Technischen Universität München. The samples from the catalytic epoxidation of cyclooctene were analyzed by GC (Hewlett–Packard GC HP 5890 Series II, FI detector, internal standard: dibutyl ether). The numbering scheme for NMR spectra assignments is given in Scheme 8.

General procedure for the syntheses of ligands 1b–1e by Claisen condensation and ring-closing reaction of the resulting 1,3-dione with hydrazine: Sodium (2.30 g, 100 mmol) was dissolved in ethanol (100 mL), the solvent was removed in vacuo, and the resulting KOEt was dissolved in THF (100 mL). To this solution, the ketone (50.0 mmol) was added, followed by the ester (50.0 mmol), both dissolved in THF (50 mL). After heating under reflux for 6 h, the solvent was removed again and the yellow-to-brownish solid was dissolved in water (50 mL). The aqueous solution was neutralized with acetic acid and extracted with diethyl ether (2 × 50 mL). The organic phase was dried over MgSO₄ and the solvent was removed in vacuo to yield the 1,3-dione. A solution of the crude 1,3-dione in ethanol (100 mL) was treated with an excess of hydrazine (80% in water) and refluxed for 5 h. The solution was evaporated and the resulting solid was purified by sublimation in vacuo.



Scheme 8. Numbering scheme for NMR data.

2-(5-Methylpyrazol-3-yl)pyridine (1b):^[11a] From acetone and *o*-picolinic acid methyl ester. Yield: 47%, pale yellow microcrystals. M.p.: 115 °C; IR (KBr): $\tilde{\nu}$ = 3202 s cm⁻¹, 3127s, 3094m, 3041m, 2981m, 2940m, 2870s, 1600vs, 1564s, 1505s, 1470s, 1439s, 1408s, 1372m, 1275m, 1250m, 1166m, 1144m, 1085s, 1050m, 1023m, 1000s, 966m, 958m, 884m, 854s, 778vs, 737s, 690m, 624s, 513m; IR (CH₂Cl₂): $\tilde{\nu}$ = 3511 w cm⁻¹, 3444s, (2 × NH); ¹H NMR (400.13 MHz, 25 °C, CDCl₃): δ = 8.60 (d, ³J_{10,11} = 4.8 Hz, 11-H), 7.66 (m, 8-H, 9-H), 7.16 (ddd, ³J_{9,10} = 6.5 Hz, ⁴J_{8,10} = 1.3 Hz, 10-H), 6.54 (br, 4-H), 2.31 (s, 3H, CH₃), NH not observed; ¹³C{¹H} NMR (100.63 MHz, 25 °C, CDCl₃): δ = 149.3 (C-7), 148.8 (C-11), 145.9 (C-3), 145.5 (C-5), 136.2 (C-9), 121.9 (C-10), 119.4 (C-8), 102.4 (C-4), 12.0 (CH₃); MS (EI, 70 eV): *m/z* (%) = 159 (100) [M⁺], 130 (68) [M⁺ - HN₂], 104 (6) [M⁺ - C₂N₂H₄], 103 (8) [M⁺ - C₂N₂H₅], 78 (7) [C₅H₄N⁺]; C₉H₉N₃ (159.2): calcd C 67.90, H 5.70, N 26.40; found C 68.01, H 5.90, N 26.48.

2-(5-Phenylpyrazol-3-yl)pyridine (1c):^[11b] From acetophenone and *o*-picolinic acid methyl ester. Yield: 50%; m.p.: 162 °C; IR (KBr): $\tilde{\nu}$ = 3244 s cm⁻¹, 3061m, 2862w, 2923m, 2853w, 1597m, 1567m, 1470s, 1450s, 1385w, 1314w, 1297w, 1175m, 1076m, 1047m, 995m, 972m, 957m, 912w, 802w, 780m, 759vs, 734w, 720w, 691w, 658w, 620w, 517w, 508w, 486; IR (CH₂Cl₂): $\tilde{\nu}$ = 3437 s cm⁻¹ (NH); ¹H NMR (400.13 MHz, 25 °C, CDCl₃): δ = 8.69 (d, ³J_{10,11} = 4.5 Hz, 11-H), 7.87 (m, 8-H, 9-H), 7.74 (d, ³J_{6,m} = 3.5 Hz, *o*-H), 7.42 (t, ³J_{m,p} = 7.5 Hz, *m*-H), 7.32 (t, *p*-H), 7.32 (dd, ³J_{9,10} = 7.5 Hz, 10-H), 7.05 (s, 4-H), NH not obs.; ¹³C{¹H} NMR (100.63 MHz, 25 °C, CDCl₃): δ = 151.6 (C-7), 149.5 (C-11), 148.6 (C-3), 144.6 (C-5), 137.0 (C-9), 132.6 (C-*r*), 128.7 (C-*o*), 128.0 (C-*p*), 125.7 (C-*m*), 122.9 (C-10), 120.1 (C-8), 100.4 (C-4); MS (EI, 70 eV): *m/z* (%) = 221 (100) [M⁺], 192 (43) [M⁺ - N₂H], 191 (20) [M⁺ - N₂H₂], 78 (6) [C₅H₄N⁺]; C₁₄H₁₁N₃ (231.3): calcd C 76.00, H 5.01, N 18.99; found C 75.40, H 5.04, N 18.83.

2-(5-Trifluoromethylpyrazol-3-yl)pyridine (1d):^[11c] From 2-acetylpyridine and trifluoroacetic acid ethyl ester. Yield: 52% of the monohydrate, pale yellow microcrystals. M.p.: 130 °C; IR (KBr): $\tilde{\nu}$ = 3297 s cm⁻¹, 3092m, 2854m, 2707m, 1598m, 1585s, 1567m, 1481m, 1440m, 1414m, 1361s, 1342m, 1288m, 1257s, 1178vs, 1137s (2 × CF), 1099w, 1078w, 1029s, 1013m, 996m, 967w, 899m, 852m, 782s, 748m; IR (CH₂Cl₂): $\tilde{\nu}$ = 3421 s cm⁻¹ (NH); ¹H NMR (400.13 MHz, 25 °C, [D₆]acetone): δ = 8.55 (ddd, ³J_{10,11} = 4.8 Hz, ⁴J_{9,11} = 1.7 Hz, ⁵J_{8,11} = 0.9 Hz, 11-H), 7.94 (dt, ³J_{8,9} = 7.1 Hz, ⁴J_{8,10} = 1.1 Hz, 8-H), 7.77 (ddd, ³J_{6,10} = 7.6 Hz, 9-H), 7.68 (br, 4-H), 7.30 (ddd, 10-H), 6.51 (br, N-H), 3.50 (s, 2H, H₂O); ¹³C{¹H} NMR (100.63 MHz, 25 °C, [D₆]acetone): δ = 152.3 (C-7), 150.6 (C-3), 149.9 (C-11), 137.1 (C-9, C-4), 125.0 (q, ¹J_{C,F} = 271.5 Hz, CF₃), 124.1 (C-10), 120.7 (C-8), 92.6 (q, ²J_{C,F} = 31.1 Hz, C-5); MS (EI, 70 eV): *m/z* (%) = 213 (100) [M⁺], 194 (10) [M⁺ - F], 165 (52) [M⁺ - HF - N₂], 145 (10) [M⁺ - 2HF - N₂], 138 (15) [M⁺ - HFNC₃], 136 (6) [C₄HF₃N₂⁺], 78 (21) [C₅H₃N⁺]; C₉H₆F₃N₃·H₂O (231.2): calcd C 46.76, H 3.49, N 18.18; found C 46.57, H 3.46, N 17.97.

2-(5-Methylpyrazol-3-yl)pyrazine (1e): From acetone and pyrazinecarboxylic acid ethyl ester. Yield: 44.1%, pale yellow microcrystals. M.p.: 118 °C; IR (KBr): $\tilde{\nu}$ = 3189s cm⁻¹, 3139s, 3113m, 3043w, 2955m, 2924s, 2876m, 2853m, 1587m, 1524s, 1506m, 1467m, 1455m, 1419m, 1376m, 1275w, 1261w, 1160m, 1147m, 1089m, 1028s, 1018s, 969m, 847m, 802m, 669m, 410m; IR (CH₂Cl₂): $\tilde{\nu}$ = 3443 s cm⁻¹ (NH); ¹H NMR (400.13 MHz, 25 °C, [D₆]acetone): δ = 12.05 (br, N-H), 9.04 (s, 8-H), 8.42 (d, ³J_{10,11} = 2.5 Hz, 10-H), 8.34 (d, 11-H), 6.57 (s, 4-H), 2.23 (s, CH₃); ¹³C{¹H} NMR (100.63 MHz, 25 °C, [D₆]acetone): δ = 145.8 (C-7, C-3), 144.8 (C-11, C-10), 143.4 (C-8, C-5), 105.0 (C-4), 12.16 (s, CH₃); MS (EI, 70 eV): *m/z* (%) = 160 (100) [M⁺], 131 (64) [M⁺ - HN₂], 106 (30) [M⁺ - C₃H₄N], 77 (21) [C₅H₃N⁺], 66 (7) [C₄H₄N⁺], 51 (46) [C₃HN⁺]; C₈H₈N₄ (160.2): calcd C 59.99, H 5.03, N 34.98; found C 59.57, H 5.24, N 35.16.

2-(4-Chloropyrazol-3-yl)pyridine (1f): Compound **1a** (1.45 g, 10.0 mmol) was dissolved in 6% HCl (100 mL) and stirred at room temperature while a saturated solution of chlorine in water (400 mL) was added in small portions over a period of 3 h. After another 2 h, ammonium acetate (15 g) was added and the pale yellow solution was neutralized with KOH. The resulting colorless precipitate was filtered off, washed with water, dried in vacuo, and purified by sublimation. Yield: 1.61 g (91%), white crystals. M.p.: 152 °C; IR (KBr): $\tilde{\nu}$ = 3414 m cm⁻¹, 3168vs, 3115s, 3045m, 2984m, 2950m, 1598s, 1572m, 1560m, 1482s, 1469m, 1411m, 1327m, 1319m, 1215w, 1152m,

1103m, 1092m (C-Cl), 1059m, 1015w, 989m, 928s, 841m, 786s, 742m, 672s, 626m, 555w; IR (CH₂Cl₂): $\tilde{\nu}$ = 3429 s cm⁻¹ (N-H); ¹H NMR (400.13 MHz, 25 °C, CDCl₃ + [D₆]DMSO): δ = 8.56 (d, ³J_{10,11} = 4.5 Hz, 11-H), 7.94 (d, ³J_{8,9} = 8.0 Hz, 8-H), 7.72 (dt, ³J_{9,10} = 8.0 Hz, ⁴J_{9,11} = 1.5 Hz, 9-H), 7.49 (s, 1H, 5-H), 7.20 (dd, 10-H), NH not det.; ¹³C{¹H} NMR (100.63 MHz, 25 °C, CDCl₃ + [D₆]DMSO): δ = 148.3 (C-11), 135.8 (C-9), 121.9 (C-10), 120.0 (C-8), 106.7 (C-4), broad (C-3), (C-5), (C-7); MS (EI, 70 eV, ³⁵Cl): *m/z* (%): 179 (100) [M⁺], 151 (15) [M⁺ - N₂], 144 (3) [M⁺ - Cl], 116 (40) [M⁺ - N₂ - Cl], 89 (33) [C₂H₂N₂Cl⁺], 78 (14) [C₅H₄N⁺]; C₈H₆ClN₃ (179.6): calcd C 53.50, H 3.37, N 23.40; found C 53.49, H 3.32, N 23.78.

2-(4-Bromopyrazol-3-yl)pyridine (1g): Compound **1a** (1.45 g, 10.0 mmol) was dissolved in 20% acetic acid (100 mL) and stirred at room temperature while bromine (1.59 g, 10.0 mmol), dissolved in glacial acetic acid (10 mL), was added over 15 min. The resulting pale yellow solution was neutralized with KOH. The colorless precipitate was filtered off, washed with water, dried in vacuo, and purified by sublimation. Yield: 1.99 g (89%), pale yellow needles. M.p.: 148 °C; IR (KBr): $\tilde{\nu}$ = 3417 m cm⁻¹, 3172vs, 3110s, 3038m, 2978w, 2945w, 2850w, 1595s, 1572m, 1555m, 1482m, 1459m, 1417w, 1407m, 1316m, 1214w, 1151w, 1105m, 1058m, 1006m (C-Br), 984m, 928s, 844m, 786s, 742m, 670s, 626w, 516w; IR (CH₂Cl₂): $\tilde{\nu}$ = 3427 s cm⁻¹ (N-H); ¹H NMR (400.13 MHz, 25 °C, CDCl₃): δ = 12.33 (br, N-H), 8.66 (d, ³J_{10,11} = 4.5 Hz, 11-H), 8.28 (d, ³J_{8,9} = 8.0 Hz, 8-H), 7.80 (dt, ³J_{9,10} = 8.0 Hz, ⁴J_{9,11} = 1.5 Hz, 9-H), 7.63 (s, 1H, 5-H), 7.29 (dd, 10-H); ¹³C{¹H} NMR (100.63 MHz, 25 °C, CDCl₃): δ = 149.4 (C-11), 146.9 (C-7), 142.1 (C-5), 138.0 (C-3), 137.1 (C-9), 123.4 (C-10), 120.6 (C-8), 92.3 (C-4); MS (EI, 70 eV, ⁷⁹Br): *m/z* (%) = 223 (75) [M⁺], 197 (5) [M⁺ - N₂], 144 (10) [M⁺ - Br], 116 (100) [M⁺ - Br - N₂], 89 (76) [C₆H₃N⁺], 78 (56) [C₅H₄N⁺]; C₈H₆BrN₃ (224.1): calcd C 42.88, H 2.70, N 18.76; found C 42.63, H 2.70, N 18.73.

2-(4-Nitropyrazol-3-yl)pyridine (1h): Compound **1a** (1.45 g, 10.0 mmol) was dissolved in 80% H₂SO₄ (10 mL) at 0 °C. To this solution, a mixture of 65% HNO₃ (5 mL) and 80% H₂SO₄ (5 mL) was added dropwise over a period of 30 min. After the reaction mixture had been heated to 90 °C for 4 h, it was poured over ice (300 g) and carefully neutralized with conc. K₂CO₃. The resulting colorless precipitate was filtered off, washed with water, dried in vacuo, and purified by sublimation. Yield: 1.18 g (62%), white microcrystals. M.p.: 167 °C; IR (KBr): $\tilde{\nu}$ = 3169 m cm⁻¹, 3139s, 3128s, 3103m, 3038m, 2968m, 2921m, 2887w, 2799w, 1594m, 1564m, 1543m, 1500s (N=O)_{as}, 1488s, 1464s, 1422s, 1386s, 1354m, 1330vs (N=O)_{sym}, 1290w, 1252w, 1216m, 1178w, 1161m, 1095m, 1065m, 1030w, 994m, 923m, 881m, 849w, 832m, 791s, 757s, 679w, 628w; IR (CH₂Cl₂): $\tilde{\nu}$ = 3401 s cm⁻¹ (N-H); ¹H NMR (400.13 MHz, 25 °C, [D₆]acetone): δ = 13.05 (br, N-H), 8.76 (d, ³J_{10,11} = 4.2 Hz, 11-H), 8.45 (br, 5-H), 8.08 (br, 8-H), 7.99 (t, ³J_{8,9} = ³J_{9,10} = 7.3 Hz, 9-H), 7.55 (t, 10-H); ¹³C{¹H} NMR (100.63 MHz, 25 °C, [D₆]acetone): δ = 149.4 (C-7), 149.3 (C-11), 149.1 (C-3), 136.8 (C-9), 132.5 (C-5), 124.4 (C-10), 124.3 (C-8), 123.6 (C-4); MS (EI, 70 eV): *m/z* (%) = 190 (55) [M⁺], 160 (2) [M⁺ - NO], 116 (37) [M⁺ - C₅H₄N], 105 (54) [C₆H₃N₂⁺], 89 (100) [C₆H₃N⁺], 78 (57) [C₅H₄N⁺]; C₈H₆N₄O₂ (190.2): calcd C 50.53, H 3.18, N 29.46; found C 50.37, H 3.25, N 29.66.

General procedure for the syntheses of the octyl derivatives 2b–e by alkylation of 1b–e with octyl iodide: NaH (0.24 g, 10 mmol) was suspended in THF (50 mL). To this suspension, the ligands **1b–e** (10 mmol) were added and the mixture was stirred until the evolution of hydrogen stopped. Then C₈H₁₇I (2.40 g, 10 mmol) was added and the resulting solution was refluxed for 24 h. After removing the solvent in vacuo, the product was extracted from the oily residue with boiling hexane. The ligands **2b–e** were obtained in 60–80% yield as oils with sufficient purity (GC, NMR) for the syntheses of the peroxo complexes.

2-(5-Methyl-1-octylpyrazol-3-yl)pyridine (2b): ¹H NMR (400.13 MHz, 25 °C, CDCl₃): δ = 8.50 (dd, ³J_{10,11} = 4.5 Hz, ⁴J_{9,11} = 2.0 Hz, 11-H), 7.79 (dd, ³J_{8,9} = 8.0 Hz, ⁴J_{8,10} = 1.0 Hz, 8-H), 7.60 (dt, ³J_{9,10} = 8.0 Hz, 9-H), 7.06 (ddd, 10-H), 6.53 (s, 4-H), 3.98 (t, ³J_{H,H} = 8.0 Hz, NCH₂), 2.24 (s, C-5-CH₃), 1.77 (br, NCH₂CH₂), 1.22–1.18 (br, 10H, CH₂), 0.80 (t, ³J_{H,H} = 6.5 Hz, CH₂CH₃); ¹³C{¹H} NMR (100.63 MHz, 25 °C, CDCl₃): δ = 152.4 (C-7), 149.8 (C-3), 149.2 (C-11), 139.2 (C-5), 136.3 (C-9), 121.9 (C-10), 119.7 (C-8), 103.7 (C-4), 49.3 (NCH₂), 31.5–22.4 (CH₂), 13.9 (CH₂CH₃), 11.1 (C-5-CH₃); MS (EI, 70 eV): *m/z* (%) = 271 (20) [M⁺], 256

(5) [$M^+ - CH_3$], 242 (9) [$M^+ - C_2H_5$], 228 (26) [$M^+ - C_3H_7$], 214 (21) [$M^+ - C_4H_9$], 200 (6) [$M^+ - C_5H_{11}$], 186 (16) [$M^+ - C_6H_{13}$], 172 (100) [$M^+ - C_7H_{15}$], 159 (35) [$M^+ - C_8H_{16}$], 145 (6) [$M^+ - C_8H_{16} - CH_3$], 130 (19) [$M^+ - C_8H_{17}N_2$], 117 (10) [$M^+ - C_8H_{16} - C_2H_4N$], 104 (8) [$M^+ - C_8H_{16} - C_2H_5N_2$], 78 (25) [$C_5H_4N^+$].

2-(1-Octyl-5-phenylpyrazol-3-yl)pyridine (2c): 1H NMR (400.13 MHz, 25 °C, $CDCl_3$): δ = 8.56 (d, $^3J_{10,11}$ = 5.0 Hz, 11-H), 7.88 (d, $^3J_{8,9}$ = 8.0 Hz, 8-H), 7.65 (t, $^3J_{9,10}$ = 8.1 Hz, 9-H), 7.39 (m, 5H, H_{Ph}), 7.11 (dd, 10-H), 6.83 (s, 4-H), 4.09 (t, $^3J_{H,H}$ = 7.8 Hz, NCH_2), 1.75 (br, NCH_2CH_2), 1.19 (br, $NCH_2CH_2CH_2$), 1.11 (br, 8H, CH_2), 0.79 (t, $^3J_{H,H}$ = 7.0 Hz, CH_3); $^{13}C\{^1H\}$ NMR (100.63 MHz, 25 °C, $CDCl_3$): δ = 152.1 (C-7), 150.3 (C-3), 149.3 (C-11), 136.1 (C-9), 130.6 (C-5), 128.7–128.2 (C_{Ph}), 122.1 (C-10), 119.9 (C-8), 104.4 (C-4), 49.7 (NCH_2), 31.5–22.4 (CH_2), 13.9 (CH_3); MS (EI, 70 eV): m/z (%) = 333 (35) [M^+], 304 (9) [$M^+ - C_2H_5$], 290 (29) [$M^+ - C_3H_7$], 276 (19) [$M^+ - C_4H_9$], 262 (3) [$M^+ - C_5H_{11}$], 249 (8) [$M^+ - C_6H_{13}$], 248 (34) [$M^+ - C_6H_{13}$], 235 (52) [$M^+ - C_7H_{15}$], 234 (100) [$M^+ - C_7H_{15}$], 222 (17) [$M^+ - C_8H_{15}$], 221 (31) [$M^+ - C_8H_{16}$], 78 (14) [$C_5H_4N^+$].

2-(1-Octyl-5-trifluoromethyl-3-pyrazolyl)pyridine (2d): 1H NMR (400.13 MHz, 25 °C, $CDCl_3$): δ = 8.52 (d, $^3J_{10,11}$ = 4.5 Hz, 11-H), 7.84 (d, $^3J_{8,9}$ = 8.0 Hz, 8-H), 7.65 (dt, $^3J_{9,10}$ = 7.8 Hz, $^4J_{9,11}$ = 1.5 Hz, 9-H), 6.15 (s, 4-H), 7.09 (dd, 10-H), 4.15 (t, $^3J_{H,H}$ = 7.5 Hz, NCH_2), 1.84 (br, NCH_2CH_2), 1.23 (br, $NCH_2CH_2CH_2$), 1.18 (br, 8H, CH_2), 0.77 (t, $^3J_{H,H}$ = 7.2 Hz, CH_3); $^{13}C\{^1H\}$ NMR (100.63 MHz, 25 °C, $CDCl_3$): δ = 151.0 (C-7), 150.5 (C-3), 149.3 (C-11), 136.3 (C-9), 133.7 (q, $^2J_{C,F}$ = 39.0 Hz, C-5), 122.6 (C-10), 119.9 (q, $^1J_{C,F}$ = 267.7 Hz, CF_3), 119.8 (C-8), 105.7 (q, $^3J_{C,F}$ = 2.0 Hz, C-4), 51.4 (NCH_2), 31.7–22.4 (CH_2), 13.8 (CH_3); MS (EI, 70 eV): m/z (%) = 325 (13) [M^+], 306 (6) [$M^+ - F$], 282 (25) [$M^+ - C_3H_7$], 268 (24) [$M^+ - F_2$], 256 (84) [$M^+ - CF_3$], 226 (100) [$M^+ - C_7H_{15}$], 213 (46) [$M^+ - C_8H_{16}$], 157 (4) [$M^+ - C_8H_{15}F_3$], 78 (25) [$C_5H_4N^+$], 51 (8) [$C_4H_3^+$].

2-(5-Methyl-1-octylpyrazol-3-yl)pyridine (2e): 1H NMR (400.13 MHz, 25 °C, $CDCl_3$): δ = 9.03 (d, $^4J_{8,10}$ = 2.5 Hz, 8-H), 8.39 (d, $^3J_{10,11}$ = 3.2 Hz, 11-H), 8.28 (dd, 10-H), 6.51 (s, 4-H), 3.96 (t, $^3J_{H,H}$ = 7.5 Hz, NCH_2), 2.19 (s, C5- CH_3), 1.73 (br, NCH_2CH_2), 1.20–1.14 (br, 10H, CH_2), 0.75 (t, $^3J_{H,H}$ = 6.5 Hz, CH_2CH_3); $^{13}C\{^1H\}$ NMR (100.63 MHz, 25 °C, $CDCl_3$): δ = 148.0 (C-7), 147.2 (C-3), 143.6, 142.3, 141.8 (C-11, C-10, C-8), 139.3 (C-5), 104.1 (C-4), 49.2 (NCH_2), 31.5–22.3 (CH_2), 13.8 (CH_2CH_3), 11.0 (C5- CH_3); MS (EI, 70 eV): m/z (%) = 272 (32) [M^+], 257 (4) [$M^+ - CH_3$], 243 (5) [$M^+ - C_2H_5$], 229 (16) [$M^+ - C_3H_7$], 215 (15) [$M^+ - C_4H_9$], 201 (3) [$M^+ - C_5H_{11}$], 188 (6) [$M^+ - C_6H_{13}$], 187 (7) [$M^+ - C_6H_{13}$], 174 (38) [$M^+ - C_7H_{15}$], 173 (100) [$M^+ - C_7H_{15}$], 160 (49) [$M^+ - C_8H_{16}$], 30 (19) [$M^+ - C_8H_{17}N_2$], 105 (8) [$M^+ - C_8H_{16} - C_2H_4N_2$], 79 (25) [$C_4H_3N_2^+$].

2-(4-Chloro-1-octylpyrazol-3-yl)pyridine (2f): Compound **2a** (2.57 g, 10.0 mmol) was dissolved in 6% HCl (100 mL) and stirred at room temperature while a saturated solution of chlorine in water (400 mL) was added in small portions over a period of 3 h. After another 2 h, ammonium acetate (15 g) was added and the pale yellow solution was neutralized with KOH. The oily product was extracted with ethyl acetate (2 × 25 mL) and dichloromethane (1 × 10 mL). The organic phase was washed with water (2 × 25 mL), dried over $MgSO_4$ and the solvent was removed in vacuo. Yield: 2.86 g (98%) colorless oil. 1H NMR (400.13 MHz, 25 °C, $CDCl_3$): δ = 8.68 (d, $^3J_{10,11}$ = 4.3 Hz, 11-H), 7.91 (d, $^3J_{8,9}$ = 7.9 Hz, 8-H), 7.68 (t, $^3J_{9,10}$ = 7.9 Hz, 9-H), 7.42 (s, 5-H), 7.19 (dd, 10-H), 4.07 (t, 3J = 7.3 Hz, NCH_2CH_2), 1.82 (quint, NCH_2CH_2), 1.28–1.20 (m, 10H, CH_2), 0.80 (t, 3J = 6.7 Hz, CH_3); $^{13}C\{^1H\}$ NMR (100.63 MHz, 25 °C, $CDCl_3$): δ = 152.0 (C-7), 150.6 (C-11), 149.8 (C-3), 136.5 (C-9), 128.9 (C-5), 122.4 (C-10), 122.0 (C-8), 108.1 (C-4), 53.1 (NCH_2), 31.6–22.4 (CH_2), 13.9 (CH_3); MS (EI, 70 eV, ^{35}Cl): m/z (%) = 291 (33) [M^+], 276 (2) [$M^+ - CH_3$], 262 (8) [$M^+ - C_2H_5$], 248 (20) [$M^+ - C_3H_7$], 234 (15) [$M^+ - C_4H_9$], 220 (14) [$M^+ - C_5H_{11}$], 206 (39) [$M^+ - C_6H_{13}$], 192 (40) [$M^+ - C_7H_{15}$], 179 (58) [$M^+ - C_8H_{16}$], 158 (5) [$M^+ - C_7H_{14} - Cl$], 144 (8) [$M^+ - C_8H_{16} - Cl$], 130 (21) [$M^+ - C_8H_{16}N - Cl$], 117 (12) [$M^+ - C_8H_{15}N_2 - Cl$], 78 (30) [$C_5H_4N^+$].

2-(4-Bromo-1-octylpyrazol-3-yl)pyridine (2g): Compound **2a** (2.57 g, 10.0 mmol) was dissolved in 20% acetic acid (100 mL) and stirred at room temperature while bromine (1.59 g, 10.0 mmol) dissolved in glacial acetic acid (10 mL) was added over 15 min. The resulting pale yellow solution was neutralized with KOH. The oily product was extracted with ethyl acetate

(2 × 25 mL). The organic phase was washed with water (2 × 25 mL) and dried over $MgSO_4$, and the solvent was removed in vacuo. Yield: 2.46 g (73%) pale yellow oil. 1H NMR (400.13 MHz, 25 °C, $CDCl_3$): δ = 8.68 (ddd, $^3J_{10,11}$ = 4.2 Hz, $^4J_{9,11}$ = 1.8 Hz, $^5J_{8,11}$ = 0.9 Hz, 11-H), 7.92 (dt, $^3J_{8,9}$ = 7.9 Hz, $^4J_{8,10}$ = 0.9 Hz, 8-H), 7.69 (dt, $^3J_{9,10}$ = 7.9 Hz, 9-H), 7.45 (s, 5-H), 7.19 (ddd, 10-H), 4.10 (t, 3J = 7.3 Hz, NCH_2CH_2), 1.89 (quint, NCH_2CH_2), 1.35–1.20 (m, 10H, CH_2), 0.82 (t, 3J = 6.9 Hz, CH_3); $^{13}C\{^1H\}$ NMR (100.63 MHz, 25 °C, $CDCl_3$): δ = 149.9 (C-7), 148.4 (C-11), 146.1 (C-3), 135.2 (C-9), 130.1 (C-5), 121.4 (C-10), 121.0 (C-8), 90.6 (C-4), 52.1 (NCH_2), 30.5–19.7 (CH_2), 12.9 (CH_3); MS (EI, 70 eV, ^{79}Br): m/z (%) = 335 (36) [M^+], 320 (5) [$M^+ - CH_3$], 306 (24) [$M^+ - C_2H_5$], 292 (66) [$M^+ - C_3H_7$], 278 (52) [$M^+ - C_4H_9$], 264 (14) [$M^+ - C_5H_{11}$], 250 (44) [$M^+ - C_6H_{13}$], 236 (91) [$M^+ - C_7H_{15}$], 223 (53) [$M^+ - C_8H_{16}$], 209 (5) [$M^+ - C_8H_{16}N$], 158 (14) [$M^+ - C_7H_{14} - Br$], 144 (8) [$M^+ - C_8H_{16} - Br$], 130 (21) [$M^+ - C_8H_{16}N - Br$], 116 (38) [$M^+ - C_8H_{16}N_2 - Br$], 78 (62) [$C_5H_4N^+$].

2-(4-Nitro-1-octylpyrazol-3-yl)pyridine (2h): Compound **2a** (2.57 g, 10.0 mmol) was dissolved in 80% H_2SO_4 (10 mL) at 0 °C. To this solution, a mixture of 65% HNO_3 (5 mL) and 80% H_2SO_4 (5 mL) was added dropwise over a period of 30 min. After the reaction mixture had been heated to 90 °C for 4 h, it was poured over ice (300 g) and carefully neutralized with conc. K_2CO_3 . The oily product was extracted with ethyl acetate (2 × 25 mL) and dichloromethane (1 × 10 mL), the organic phase was washed with water (2 × 25 mL), dried over $MgSO_4$ and the solvent was removed in vacuo. Yield: 2.12 g (70%), yellow oil. 1H NMR (400.13 MHz, 25 °C, $CDCl_3$): δ = 8.66 (d, $^3J_{10,11}$ = 4.5 Hz, 11-H), 8.19 (s, 5-H), 7.72 (dt, $^3J_{8,9}$ = $^3J_{9,10}$ = 7.5 Hz, $^4J_{9,11}$ = 1.5 Hz, 9-H), 7.66 (d, 8-H), 7.19 (ddd, $^4J_{8,10}$ = 1.5 Hz, 10-H), 4.11 (t, 3J = 7.3 Hz, NCH_2CH_2), 1.86 (quint, NCH_2CH_2), 1.25–1.15 (m, 10H, CH_2), 0.79 (t, 3J = 6.9 Hz, CH_3); $^{13}C\{^1H\}$ NMR (100.63 MHz, 25 °C, $CDCl_3$): δ = 149.4 (C-11), 149.0 (C-7), 146.0 (C-3), 136.1 (C-9), 132.7 (C-4), 130.2 (C-5), 124.7 (C-10), 123.7 (C-8), 53.5 (NCH_2), 31.5–22.3 (CH_2), 13.8 (CH_3); MS (EI, 70 eV): m/z (%) = 302 (5) [M^+], 301 (5) [$M^+ - H$], 287 (12) [$M^+ - CH_3$], 285 (100) [$M^+ - OH$], 273 (29) [$M^+ - C_2H_5$], 259 (29) [$M^+ - C_3H_7$], 245 (22) [$M^+ - C_4H_9$], 231 (18) [$M^+ - C_5H_{11}$], 217 (39) [$M^+ - C_6H_{13}$], 203 (64) [$M^+ - C_7H_{15}$], 190 (29) [$M^+ - C_8H_{16}$], 105 (30) [$C_5H_5N^+$], 78 (41) [$C_5H_4N^+$].

Syntheses of the peroxy complexes **3b–h**:

Method A: A solution of an octyl-substituted pyrazolopyridine (**2b–h**, 3.00 mmol) in methanol (30 mL) was added to a solution of molybdic acid (0.97 g, 6.00 mmol) in 30% H_2O_2 (30 mL), and the resulting mixtures were vigorously stirred for 10 min. The complexes were extracted with CH_2Cl_2 (2 × 50 mL). To remove traces of H_2O_2 , the combined organic solutions were washed with water (2 × 50 mL) and dried over $MgSO_4$. Evaporation of the solvent yielded yellow solids, which were washed with Et_2O (2 × 30 mL) to remove organic impurities.

Method B: A solution of an octyl-substituted pyrazolopyridine (**2b–h**, 3.00 mmol) in CH_2Cl_2 (20 mL) was added to a solution of $[MoO(O_2)_2(DMF)_2]$ (1.93 g, 6.00 mmol) in CH_2Cl_2 (30 mL) and the resulting mixture was stirred for 1 h. The solvent was evaporated to dryness and the resulting yellow solids were extracted with diethyl ether (2 × 20 mL) to remove organic impurities. Extraction with hot ethyl acetate and evaporation of the yellow solutions yielded the desired peroxy complexes. Isolated yields of peroxy complexes: 60–80%, yellow microcrystalline solids.

[2-(5-Methyl-1-octylpyrazol-3-yl)pyridine]oxodiperoxo molybdenum (vi) (3b): IR (KBr): $\tilde{\nu}$ = 3134 cm^{-1} , 3086 w, 3059 w, 2955 s, 2917 vs, 2868 s, 2851 s, 1611 s, 1567 w, 1517 m, 1467 s, 1459 s, 1443 s, 1424 s, 1379 s, 1327 m, 1290 w, 1252 w, 1217 m, 1160 m, 1111 m, 1054 m, 1025 w, 949 vs ($Mo=O$), 878 s, 866 vs (2 × O–O), 820 m, 788 vs, 752 w, 658 s, 643 m, 585 s, 538 m; 1H NMR (400.13 MHz, 25 °C, $CDCl_3$): isomer A: δ = 9.16 (d, $^3J_{10,11}$ = 6.0 Hz, 11-H), 8.17 (t, $^3J_{8,9}$ = $^3J_{9,10}$ = 6.4 Hz, 9-H), 7.86 (d, 8-H), 7.58 (t, 10-H), 6.46 (s, 4-H), 3.98 (t, $^3J_{H,H}$ = 8.0 Hz, NCH_2CH_2), 2.19 (s, C5- CH_3), 1.62 (br, NCH_2CH_2), 1.3–1.1 (m, 10H, CH_2), 0.80 (t, $^3J_{H,H}$ = 7.0 Hz, CH_3); isomer B: δ = 8.15 (d, $^3J_{10,11}$ = 4.5 Hz, 11-H), 7.74 (t, $^3J_{8,9}$ = $^3J_{9,10}$ = 7.5 Hz, 9-H), 7.59 (d, 8-H), 7.16 (t, 10-H), 6.82 (s, 4-H), 4.55 (t, $^3J_{H,H}$ = 7.5 Hz, NCH_2), 2.53 (s, C5- CH_3), 1.97 (br, NCH_2CH_2), 1.3–1.1 (m, 10H, CH_2), 0.82 (t, $^3J_{H,H}$ = 7.0 Hz, CH_3); isomer ratio A/B: 0.98; $^{13}C\{^1H\}$ NMR (100.63 MHz, 25 °C, $CDCl_3$): isomer A: δ = 154.3 (C-11), 151.1 (C-7), 146.8 (C-3), 143.8 (C-5), 142.8 (C-9), 125.8 (C-10), 122.4 (C-8), 103.8 (C-4), 49.5 (NCH_2), 31.6–22.4 (CH_2), 14.0 (CH_3), 11.1 (C5- CH_3); isomer B: δ = 151.1

(C-7), 147.4 (C-3), 146.8 (C-11), 145.0 (C-5), 139.0 (C-9), 124.8 (C-10), 120.4 (C-8), 105.2 (C-4), 49.5 (NCH₂), 31.6–22.4 (CH₂), 14.0 (CH₃), 12.3 (C-5-CH₃); C₁₇H₂₃MoN₃O₅ (447.4): calcd C 45.64, H 5.63, N 9.39; found C 45.42, H 5.51, N 9.28.

[2-(1-Octyl-5-phenylpyrazol-3-yl)pyridine]oxodiperoxomolybdenum (vi) (3c): IR (KBr): $\tilde{\nu}$ = 3124 w cm⁻¹, 3094 w, 3062 w, 3031 w, 2953 s, 2924 vs, 2854 s, 1613 s, 1567 m, 1521 m, 1483 m, 1460 s, 1438 s, 1379 m, 1341 w, 1294 w, 1250 w, 1160 w, 1112 m, 1062 m, 1027 w, 1015 m, 974 m, 952 vs (Mo=O), 876 s, 864 vs (2 × O–O), 784 s, 765 s, 700 s, 678 m, 663 s, 584 s, 535 m; ¹H NMR (400.13 MHz, 25 °C, CDCl₃): isomer A: δ = 9.19 (d, ³J_{10,11} = 5.5 Hz, 11-H), 8.20 (t, ³J_{8,9} = ³J_{9,10} = 7.0 Hz, 9-H), 7.93 (d, 8-H), 7.59 (t, 10-H), 6.63 (s, 4-H), 4.06 (t, ³J_{H,H} = 7.8 Hz, NCH₂CH₂), 1.48 (br, NCH₂CH₂), 1.2–1.0 (m, 10-H, CH₂), 0.75 (t, ³J_{H,H} = 7.8 Hz, CH₃); isomer B: δ = 8.18 (d, ³J_{10,11} = 3.0 Hz, 11-H), 7.76 (t, ³J_{8,9} = ³J_{9,10} = 7.8 Hz, 9-H), 7.63 (d, 8-H), 7.18 (t, 10-H), 6.95 (s, 4-H), 4.59 (t, ³J_{H,H} = 7.5 Hz, NCH₂), 1.95 (br, NCH₂CH₂), 1.2–1.0 (m, 10-H, CH₂), 0.76 (t, ³J_{H,H} = 7.8 Hz, CH₃); isomer ratio A/B: 1.42; ¹³C{¹H} NMR (100.63 MHz, 25 °C, CDCl₃): isomer A: δ = 154.4 (C-11), 150.9 (C-7), 146.6 (C-3), 144.3 (C-5), 142.8 (C-9), 131.7–127.7 (C_{ph}), 125.0 (C-10), 122.6 (C-8), 104.5 (C-4), 50.0 (NCH₂), 31.5–22.4 (CH₂), 14.0 (CH₃); isomer B: δ = 151.7 (C-3, C-7), 147.0 (C-11), 144.9 (C-5), 139.1 (C-9), 131.7–127.7 (C_{ph}), 125.0 (C-10), 120.5 (C-8), 105.5 (C-4), 50.0 (NCH₂), 31.5–22.4 (CH₂), 14.0 (CH₃); C₂₂H₂₇MoN₃O₅ (509.4): calcd C 51.87, H 5.34, N 8.25; found C 51.64, H 5.18, N 8.17.

2-(1-Octyl-5-trifluoromethyl-3-pyrazolyl)pyridineoxodiperoxomolybdenum(vi) (3d): IR (KBr): $\tilde{\nu}$ = 3121 m cm⁻¹, 3092 w, 2954 m, 2927 s, 2858 m, 1612 m, 1558 w, 1442 m, 1417 w, 1383 w, 1347 m, 1275 s, 1217 m, 1174 vs, 1141 vs (2 × CF), 1087 w, 1061 m, 1041 w, 1028 w, 963 s (Mo=O), 880 m, 870 s (2 × O–O), 842 w, 788 s, 750 w, 729 w, 696 w, 668 m, 592 m, 544 w; ¹H NMR (400.13 MHz, 25 °C, CDCl₃): isomer A: δ = 9.28 (d, ³J_{10,11} = 5.5 Hz, 11-H), 8.30 (dt, ³J_{8,9} = ³J_{9,10} = 8.0 Hz, ⁴J_{9,11} = 1.5 Hz, 9-H), 7.99 (d, 8-H), 7.72 (dd, 10-H), 7.05 (s, 4-H), 4.21 (t, ³J_{H,H} = 8.3 Hz, NCH₂), 1.75 (m, NCH₂CH₂), 1.4–1.3 (m, 10-H, CH₂), 0.85 (t, ³J_{H,H} = 6.3 Hz, CH₃); isomer B: δ = 8.25 (d, ³J_{10,11} = 4.0 Hz, 11-H), 7.86 (t, ³J_{8,9} = ³J_{9,10} = 8.2 Hz, 9-H), 7.70 (d, 8-H), 7.32 (s, 4-H), 7.28 (dd, 10-H), 4.78 (t, ³J_{H,H} = 7.3 Hz, NCH₂), 2.12 (m, NCH₂CH₂), 1.3–1.2 (m, 10-H, CH₂), 0.82 (t, ³J_{H,H} = 6.3 Hz, CH₃); isomer ratio A/B: 28.9; ¹³C{¹H} NMR (100.63 MHz, 25 °C, CDCl₃): isomer A: δ = 155.0 (C-11), 149.7 (C-7), 144.2 (C-3), 143.2 (C-9), 134.5 (q, ²J_{C,F} = 40.8 Hz, C-5), 125.9 (C-10), 123.0 (C-8), 118.6 (q, ¹J_{C,F} = 270.2 Hz, CF₃), 105.4 (q, ³J_{C,F} = 3.1 Hz, C-4), 52.4 (NCH₂), 31.7–22.6 (CH₂), 14.0 (CH₃); isomer B: no signals identified; ¹⁹F{¹H} NMR (376.48 MHz, 25 °C, CDCl₃): isomer A: δ = 2.35 (s, CF₃), isomer B: δ = 2.05 (s, CF₃), isomer ratio A/B: 23.4; C₁₇H₂₂F₃MoN₃O₅ (501.3): calcd C 40.73, H 4.42, N 8.38; found C 39.67, H 4.35, N 8.11.

2-(5-Methyl-1-octylpyrazol-3-yl)pyrazineoxodiperoxomolybdenum(vi) (3e): IR (KBr): $\tilde{\nu}$ = 3122 w cm⁻¹, 3074 w, 2955 s, 2926 vs, 2854 s, 1532 m, 1458 s, 1426 s, 1406 s, 1367 m, 1226 w, 1172 m, 1162 s, 1110 w, 1108 w, 1058 m, 1044 s, 959 vs, 944 vs (2 × Mo=O), 868 vs (O–O), 825 w, 662 m, 644 w, 586 s, 542 m; ¹H NMR (400.13 MHz, 25 °C, CDCl₃): isomer A: δ = 9.23 (d, ⁴J_{8,10} = 1.0 Hz, 8-H), 9.12 (dd, ³J_{10,11} = 3.0 Hz, 10-H), 8.94 (d, 11-H), 6.60 (s, 4-H), 3.96 (t, ³J_{H,H} = 8.0 Hz, NCH₂), 2.24 (s, C5–CH₃), 1.99 (br, NCH₂CH₂), 1.30–1.13 (br, 10-H, CH₂), 0.80 (t, ³J_{H,H} = 6.5 Hz, CH₂CH₃); isomer B: δ = 8.92 (d, ⁴J_{8,10} = 1.5 Hz, 8-H), 8.52 (d, ³J_{10,11} = 2.5 Hz, 11-H), 8.15 (dd, 10-H), 6.95 (s, 4-H), 4.59 (t, ³J_{H,H} = 7.5 Hz, NCH₂), 2.58 (s, C5–CH₃), 1.99 (br, NCH₂CH₂), 1.30–1.13 (br, 10-H, CH₂), 0.80 (t, ³J_{H,H} = 6.5 Hz, CH₂CH₃); isomer ratio A/B: 0.084; ¹³C{¹H} NMR (100.63 MHz, 25 °C, CDCl₃): isomer A: δ = 146.2, 145.8, 145.2, 144.5, 142.6, 141.2 (C-3, C-5, C-7, C-8, C-10, C-11), 104.4 (C-4), 49.9 (NCH₂), 31.6–22.5 (CH₂), 13.9 (CH₂CH₃), 11.2 (C5–CH₃); isomer B: δ = 148.5 (C-3), 147.8 (C-7), 146.2, 141.2, 140.1 (C-11, C-10, C-8), 140.3 (C-5), 105.7 (C-4), 49.8 (NCH₂), 31.6–22.5 (CH₂), 13.9 (CH₂CH₃), 12.4 (C5–CH₃); C₁₆H₂₄MoN₄O₅ (448.34): calcd C 42.86, H 5.40, N 12.50; found C 42.37, H 5.41, N 12.53.

2-(4-Chloro-1-octyl-3-pyrazolyl)pyridineoxodiperoxomolybdenum(vi) (3f): IR (KBr): $\tilde{\nu}$ = 3132 m cm⁻¹, 3120 m, 2954 s, 2924 vs, 2854 s, 1611 s, 1566 w, 1522 m, 1467 m, 1435 s, 1373 m, 1334 m, 1290 w, 1251 w, 1217 m, 1166 m, 1122 w, 1109 w, 1065 m, 1056 m, 1032 w, 1002 m (C–Cl), 956 vs, 947 vs (2 × Mo=O), 878 s, 865 vs (2 × O–O), 881 m, 790 s, 754 m, 690 w, 666 m, 635 m, 588 s, 534 m; ¹H NMR (400.13 MHz, 25 °C, CDCl₃): isomer A: δ = 9.35 (d, ³J_{10,11} = 5.5 Hz, 11-H), 8.59 (d, ³J_{8,9} = 7.6 Hz, 8-H), 8.27 (dt, ³J_{8,9} = 7.5 Hz, ⁴J_{9,11} = 1.5 Hz, 9-H), 7.69 (ddd, ⁴J_{8,10} = 1.5 Hz, 10-H), 7.38

(s, 5-H), 4.14 (t, ³J_{H,H} = 7.3 Hz, NCH₂CH₂), 1.73 (br, NCH₂CH₂), 1.30–1.20 (m, 10-H, CH₂), 0.81 (t, ³J_{H,H} = 6.9 Hz, CH₃); isomer B: δ = 8.41 (d, ³J_{10,11} = 4.0 Hz, 11-H), 8.26 (br, 8-H), 8.05 (s, 5-H), 7.86 (dt, ³J_{8,9} = ³J_{9,10} = 7.8 Hz, ⁴J_{9,11} = 1.5 Hz, 9-H), 7.30 (dd, 10-H), 4.69 (t, ³J_{H,H} = 7.3 Hz, NCH₂CH₂), 2.06 (br, 2H, NCH₂CH₂), 1.30–1.20 (m, 10-H, CH₂), 0.81 (t, ³J_{H,H} = 6.9 Hz, 3H, CH₃); isomer ratio A/B: 7.05; ¹³C{¹H} NMR (100.63 MHz, 25 °C, CDCl₃): isomer A: δ = 155.1 (C-11), 149.8 (C-7), 142.9 (C-9), 149.6 (C-3), 130.8 (C-5), 125.5 (C-10), 123.4 (C-8), 109.7 (C-4), 53.06 (NCH₂), 32.0–22.5 (CH₂), 14.03 (CH₃); isomer B: δ = 155.0 (C-3), 147.5 (C-11), 143.8 (C-7), 139.2 (C-9), 136.6 (C-5), 123.4 (C-10), 121.5 (C-8), 110.6 (C-4), 53.97 (NCH₂), 32.0–21.5 (CH₂), 14.03 (CH₃); C₁₆H₂₂ClMoN₃O₅ (467.78): calcd C 41.08, H 4.74, N 8.98; found C 40.64, H 4.92, N 8.91.

2-(4-Bromo-1-octyl-3-pyrazolyl)pyridineoxodiperoxomolybdenum(vi) (3g): IR (KBr): $\tilde{\nu}$ = 3103 s cm⁻¹, 2952 s, 2923 vs, 2853 s, 1612 s, 1594 w, 1568 w, 1522 w, 1506 w, 1464 m, 1436 m, 1430 m, 1370 w, 1334 w, 1261 w, 1251 w, 1207 w, 1156 w, 1108 w, 1068 w, 1056 w, 1031 w, 992 w (C–Br), 954 vs (Mo=O), 878 m, 863 vs (2 × O–O), 788 m, 751 w, 690 w, 666 m, 634 w, 587 m, 541 w; ¹H NMR (400.13 MHz, 25 °C, CDCl₃): isomer A: δ = 9.30 (dd, ³J_{10,11} = 5.5 Hz, ⁴J_{9,11} = 5.5 Hz, 11-H), 8.69 (d, ³J_{8,9} = 7.6 Hz, 8-H), 8.25 (dt, ³J_{8,9} = 7.5 Hz, 9-H), 7.68 (ddd, ⁴J_{8,10} = 1.5 Hz, 10-H), 7.37 (s, 5-H), 4.10 (t, ³J_{H,H} = 7.3 Hz, NCH₂CH₂), 1.69 (br, NCH₂CH₂), 1.30–1.20 (m, 10-H, CH₂), 0.81 (t, ³J_{H,H} = 6.9 Hz, CH₃); isomer B: δ = 8.38 (d, ³J_{10,11} = 8.0 Hz, 11-H), 8.03 (s, 5-H), 7.92 (d, ³J_{8,9} = 7.9 Hz, 8-H), 7.82 (dt, ³J_{8,9} = 7.9 Hz, 9-H), 7.69 (dd, 10-H), 4.66 (t, ³J_{H,H} = 7.3 Hz, NCH₂CH₂), 2.01 (br, NCH₂CH₂), 1.30–1.20 (m, 10-H, CH₂), 0.81 (t, ³J_{H,H} = 6.9 Hz, CH₃); isomer ratio A/B: 7.86; ¹³C{¹H} NMR (100.63 MHz, 25 °C, CDCl₃): isomer A: δ = 155.1 (C-11), 150.1 (C-7), 144.1 (C-9), 140.9 (C-3), 133.2 (C-5), 125.5 (C-10), 123.2 (C-8), 92.82 (C-4), 53.00 (NCH₂), 32.0–21.5 (CH₂), 14.03 (CH₃); isomer B: δ = 155.0 (C-3), 148.9 (C-7), 147.5 (C-11), 144.1 (C-9), 139.1 (C-5), 122.6 (C-10), 121.4 (C-8), 93.64 (C-4), 53.93 (NCH₂), 32.0–21.5 (CH₂), 14.03 (CH₃); C₁₆H₂₂BrMoN₃O₅ (512.2): calcd C 37.52, H 4.33, N 8.20; found C 37.98, H 4.37, N 8.40.

2-(4-Nitro-1-octyl-3-pyrazolyl)pyridineoxodiperoxomolybdenum(vi) (3h): IR (KBr): $\tilde{\nu}$ = 3139 m cm⁻¹, 3101 m, 2953 s, 2926 vs, 2855 s, 1619 m, 1570 m, 1540 vs, 1504 vs (N=O)_{as}, 1453 s, 1442 s, 1369 s, 1350 vs (N=O)_{sym}, 1224 m, 1147 w, 1112 w, 1038 w, 957 vs (Mo=O), 875 m, 864 vs (2 × O–O), 835 s, 790 m, 755 s, 666 m, 635 w, 617 w, 585 s, 536 m; ¹H NMR (400.13 MHz, 25 °C, CDCl₃): isomer A: δ = 9.43 (br, 11-H), 9.10 (d, ³J_{8,9} = 8.0 Hz, 8-H), 8.39 (t, ³J_{8,9} = 8.0 Hz, 9-H), 8.23 (s, 5-H), 7.86 (t, ⁴J_{10,11} = 6.3 Hz, 10-H), 4.23 (t, ³J_{H,H} = 7.0 Hz, NCH₂CH₂), 1.78 (br, NCH₂CH₂), 1.31–1.20 (m, 10-H, CH₂), 0.84 (t, ³J_{H,H} = 7.0 Hz, CH₃); isomer B: δ not detectable; isomer ratio A/B: > 50; ¹³C{¹H} NMR (100.63 MHz, 25 °C, CDCl₃): isomer A: δ = 155.6 (C-11), 147.5 (C-7), 147.5 (C-3), 143.4 (C-9), 138.6 (C-5), 133.9 (C-4), 127.4 (C-10), 127.1 (C-8), 53.6 (NCH₂), 31.6–22.5 (CH₂), 14.0 (CH₃); isomer B: δ not detectable; C₁₆H₂₂MoN₄O₇ (478.31): calcd C 40.18, H 4.64, N 11.71; found C 39.07, H 4.59, N 11.59.

Catalytic epoxidation of cyclooctene: The reactions were carried out in a two-neck 100 mL flask equipped with a reflux condenser and a Quickfit® septum adapter. In this flask cyclooctene (1.00 g, 9.07 mmol), dibutyl ether (1.00 g, 7.75 mmol, internal standard) and *t*BuOOH (1.35 mL of a 6.90 M solution in CHCl₃) were dissolved in CHCl₃ (23 mL). The solution was heated to reflux temperature (61 °C, oil bath temperature: 95 °C) and the catalysts (12–13 mg) dissolved in CHCl₃ (2 mL) were added from a PE syringe. Samples were taken after 2, 5, 10, 20, and 40 min with a PE syringe.

Acknowledgments: We thank Prof. Dr. Dr. h.c. W. A. Herrmann, the Deutsche Forschungsgemeinschaft (Schwerpunktprogramm "Peroxidchemie") and the Fonds der Chemischen Industrie for support of our work, R. Schmid for helpful discussions, and Michaela Angst for experimental help.

Received: October 21, 1996 [F 503]

- [1] W. R. Thiel, *J. Mol. Catal. A Chem.* **1997**, *117*, 449.
 [2] a) *Catalytic Oxidations with Hydrogen Peroxide as Oxidant* (Ed.: G. Strukul), Kluwer Academic, Rotterdam, **1992**; b) K. A. Jørgensen, *Chem. Rev.* **1989**, *89*, 431; c) *Organic Synthesis by Oxidation with Metal Compounds* (Ed.: W. J. Mijs, C. H. R. I. de Jonge), Plenum, New York, **1986**; d) R. A. Sheldon, J. A. Kochi, in *Metal-Catalyzed Oxidations of Organic Compounds*, Academic Press, New York, **1981**; e) R. A. Sheldon in *The Chemistry of Peroxides* (Ed.: S. Patai), Wiley, New York, 1983, p. 161.

- [3] a) R. A. Sheldon, J. A. van Doorn, *J. Catal.* **1973**, *31*, 427; b) R. A. Sheldon, J. A. van Doorn, C. W. A. Schram, A. J. de Jong, *ibid.* **1973**, *31*, 438; c) A. O. Chong, K. B. Sharpless, *J. Org. Chem.* **1977**, *42*, 1587; d) M. K. Trost, R. G. Bergman, *Organometallics* **1991**, *10*, 1172; e) P. Chaumette, H. Mimoun, L. Saussine, J. Fischer, A. Mitschler, *J. Organomet. Chem.* **1983**, *250*, 291.
- [4] a) R. A. Sheldon, *Rec. Trav. Chim. Pays-Bas* **1973**, *92*, 253; b) *ibid.*, 367.
- [5] H. Mimoun, I. Sere de Roch. L. Sajus, *Bull. Soc. Chim. Fr.* **1969**, *36*, 1481.
- [6] W. R. Thiel, M. Angstl, T. Priermeier, *Chem. Ber.* **1994**, *127*, 2373.
- [7] W. R. Thiel, T. Priermeier, *Angew. Chem.* **1995**, *107*, 1870; *Angew. Chem. Int. Ed. Engl.* **1995**, *34*, 1737.
- [8] R. Fusco in *The Chemistry of Heterocyclic Compounds: Pyrazoles, Pyrazolines, Pyrazolidines, Indazoles and Condensed Rings* (Ed.: R. H. Wiley), vol. 22, p. 1–174, Wiley, New York, **1967**.
- [9] J. Elguero in *Comprehensive Heterocyclic Chemistry* (Ed.: K. T. Potts), vol. 5, p. 291–298, Pergamon, Oxford, **1984**.
- [10] H. Brunner, T. Scheck, *Chem. Ber.* **1992**, *125*, 701.
- [11] a) M. Ferles, S. Kafka, A. Silhankova, M. Sputova, *Collect. Czech. Chem. Commun.* **1981**, *46*, 1167; b) H. Hennig, *J. Prakt. Chem.* **1966**, *306*, 64; c) US Pat. 3200128, CA **1965**, *63*, 13272b.
- [12] For the sake of simplicity, **1e** is discussed as a pyrazolylpyridine despite the fact that it contains a pyrazine instead of a pyridine system.
- [13] M. A. Khan, A. A. A. Pinto, *J. Heterocycl. Chem.* **1981**, *18*, 9.
- [14] AM1 calculations were carried out with the MOPAC 6.0 package in combination with the INSIGHTII graphical user interface (Biosym) on a Silicon Graphics 4D25 workstation. AM1 and parameters used for calculations: a) M. J. S. Dewar, E. G. Zoebisch, E. F. Healy, J. J. P. Stewart, *J. Am. Chem. Soc.* **1985**, *107*, 3902; b) M. J. S. Dewar, E. G. Zoebisch, *Theochem* **1988**, *49*, 1; c) M. J. S. Dewar, C. Jie, E. G. Zoebisch, *Organometallics* **1988**, *7*, 513.
- [15] a) A. R. Kratitzky, J. M. Logowsky in *Comprehensive Heterocyclic Chemistry* (Ed.: K. T. Potts), vol. 5, p. 35–38, Pergamon, Oxford, **1984**; b) J. Elguero in *Comprehensive Heterocyclic Chemistry* (Ed.: K. T. Potts), vol. 5, p. 211–213, Pergamon, Oxford, **1984**.
- [16] On the barrier of rotation in 2,2'-bipyridine see: Y. S. Mangutova, L. S. Mal'tseva, F. G. Kamaev, B. V. Leont'ev, S. Mikhamedkhanova, O. S. Otroschenko, A. S. Sadykov, *Izv. Akad. Nauk. SSSR. Ser. Khim.* **1973**, 1510; *Bull. Acad. Sci. SSSR. Chem. Ser.* **1973**, *22*, 1466.
- [17] a) H. A. Staab, *Einführung in die Theoretische Organische Chemie*, 4th Ed., Verlag Chemie, **1970**; b) H. A. Staab, W. Otting, A. Ueberle, *Z. Elektrochem.* **1957**, *61*, 1000; c) N. Fuson, M.-L. Josien, E. M. Shelton, *J. Am. Chem. Soc.* **1954**, *76*, 2526; d) J. Tanaka, S. Nagakura, M. Kobayashi, *J. Chem. Physics* **1956**, *24*, 311; e) C. Hansch, A. Leo, *Substituent Constants for Correlation Analysis in Chemistry and Biology*, Wiley, New York, **1979**.
- [18] W. R. Thiel, M. Angstl, N. Hansen, *J. Mol. Catal. A. Chem.* **1995**, *103*, 5.
- [19] W. R. Thiel, M. Mattner, unpublished results.
- [20] a) J. Elguero, E. Gonzalez, R. Jacquier, *Bull. Soc. Chim. Fr.* **1968**, *35*, 5009; b) J. Bjerrum, *Acta Chem. Scand.* **1964**, *18*, 843.
- [21] W. R. Thiel, *Chem. Ber.* **1996**, *129*, 575.
- [22] a) G. Boche, K. Möbus, K. Harms, M. Marsch, *J. Am. Chem. Soc.* **1996**, *118*, 2770; b) Y. D. Wu, D. K. W. Lei, *ibid.* **1995**, *117*, 11327; c) Y. D. Wu, D. K. W. Lei, *J. Org. Chem.* **1995**, *60*, 673; d) G. Boche, F. Bosold, J. C. W. Lohrenz, *Angew. Chem.* **1994**, *106*, 1228; *Angew. Chem. Int. Ed. Engl.* **1994**, *33*, 1161; e) R. D. Bach, M.-D. Su, J. L. Andrés, H. B. Schlegel, *J. Am. Chem. Soc.* **1993**, *115*, 8763.